Hindawi
Journal of Advanced Transportation
Volume 2020, Article ID 7539829, 14 pages
https://doi.org/10.1155/2020/7539829

Research Article

The Impact of Violations of Bicycles and Pedestrians on Vehicle Emissions at Signalized Intersections

Jianchang Huang, Guohua Song, Jianbo Zhang, Chenxu Li, Qiumei Liu, and Lei Yu

Key Laboratory of Transport Industry of Big Data Application Technologies for Comprehensive Transport, Beijing Jiaotong University, Beijing 100044, China

Correspondence should be addressed to Guohua Song; ghsong@bjtu.edu.cn

Received 23 September 2019; Revised 10 January 2020; Accepted 5 February 2020; Published 21 March 2020

Guest Editor: Young-Ji Byon

An intersection is a typical emission hot spot in the urban traffic network. And frequent violations such as running the red light have been a critical social problem at signalized intersections in developing countries. This article aimed to quantify the impact of violations (behaviors which will block the fleet) on emissions at signalized intersections. Increased emissions of vehicles affected by violations are of two levels: (1) trajectory level for the first four affected vehicles and (2) traffic flow level for the subsequent vehicles. At the trajectory level, the study focuses on the second-by-second activities of the first four affected vehicles. First, the trajectory model of the first affected vehicle is developed. Then, the trajectory of the other three vehicles is constructed using the Gipps car-following model. At the traffic flow level, a linear emission model is developed to describe the relationship between emission factors and idling time in the one-stop (vehicle stop once) and two-stop (vehicle stop twice) scenarios based on the global position system (GPS)-collected data at 44 intersections in Beijing. Based on the linear emission model, increased emissions at the traffic flow level are calculated as knowing the number of stops and idling time before and after violations. The analysis of the subsequent vehicles is divided into unsaturated and saturated conditions. Under the unsaturated condition, the emissions have barely increased due to the increase of idling time for one-stop vehicles caused by the violations. Under the saturated conditions, the emission increment increases sharply as the one-stop vehicle gradually transforms to a two-stop vehicle because of violations, and the maximum emission increment reaches 45% in half an hour in the case. The increment of emissions decreases steadily as the proportion of two-stop vehicles reaches 100% after violations, while the proportion before violations keeps increasing.

1. Introduction

In recent years, urban vehicle pollution has threatened human health. Air pollutants can cause pulmonary and cardiovascular diseases and chronic obstructive pulmonary disease, and decrease lung function [1]. According to the WHO report, air pollution resulted in 3.7 million premature deaths worldwide in 2012 [2]. In the United States, motorized vehicles are responsible for 57% of emissions [3].

An intersection is a typical emission hot spot in the urban traffic network [4], especially in a densely populated metropolis like Beijing. Extensive studies have been carried out on vehicle emissions around intersections, and illustrate that high emissions at intersections mainly resulted from unstable traffic operation and stop-and-go vehicle activity [5–7] and lead to high pollutant exposure, particularly to pedestrians and cyclists around the intersections.

When vehicles, pedestrians, and cyclists arrive at the intersection, each traffic subject follows the corresponding rules and passes through the intersection orderly. However, violation behaviors, one of the core factors, are frequently observed in developing countries such as China [8]. Frequent violations will not only aggravate traffic risk but also worsen the stop-and-go condition of vehicles. Four typical violations at intersections are shown in Figure 1 frequent violations of pedestrians and bicycles block the vehicle fleet, aggravating stop-and-go behaviors at intersections. In this article, the critical problem of quantifying emission increments caused by violations has been discussed.

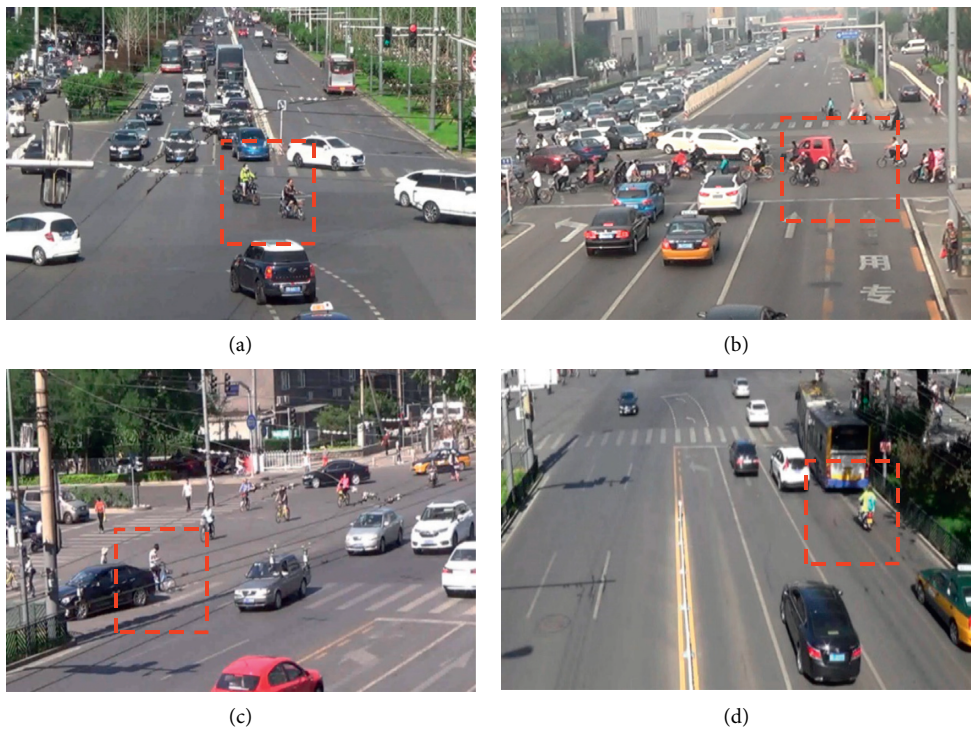

(a) (b) (c) (d)

Figure 1: Violations at signalized intersections under mixed traffic in Beijing. (a) Crossing the intersection diagonally. (b) Running the red light. (c) Waiting in front of the motorway. (d) Intruding into the lane.

Motor vehicles, bicycles, and pedestrians are three typical traffic components of mixed traffic flow intersections. Their relationships are variable and complex due to the conflict in time and space. Existing studies indicated that violations were frequently observed in developing countries and had a significant impact on driving operation [7]. Researches on the impact of violations on emissions can be summarized into two categories: (1) intersection emission estimation and (2) violation characteristics and impact analysis.

In terms of intersection emission estimation, existing studies indicated that steady speed, shortest delays, and fewest stops are the best operations for emission reduction [9, 10]; nonsmooth traffic operations and stop-and-go activity were the main reasons for high emissions at intersections; and much more time was spent in the acceleration mode after highly interrupted movements of vehicles [11–13]. During the acceleration period, an engine operates at a high level, which leads to excessive fuel consumption and emissions [14, 15]. In existing studies, extensive studies have been carried out on vehicle emission around intersections. Rakha and Ding analyzed the impact of stops on vehicle fuel consumption and emissions and found that vehicle fuel consumption was more sensitive to cruise-speed levels [13]. Papson et al. used a time-in-mode model with MOVES to analyze vehicle emissions at congested and uncongested signalized intersections [16]. Zhang et al. developed the SIDRA model to estimate intersection emissions with MOVES, and acceleration mode included constant acceleration and linearly decreasing acceleration (3). Gokhale and Pandian developed a semi-empirical box model to predict CO concentration based on the assumed traffic flow pattern at intersections [17]. Braven et al. estimated vehicle emissions at a signalized intersection by using VISSIM [18].

In terms of violation characteristic analysis, it can be summarized into two categories. (1) Violation characteristics mainly include two aspects: (a) for the influencing factors (waiting time, group size of pedestrians, gender, nonmotor vehicle type, and so on), existing studies indicated that these factors had an obvious impact on intersection violations [19–21], and (b) for the frequency model, violation probability model [22] and violation waiting time model [23] were developed to predict the frequency of violations. (2) Impact of interference has an impact on vehicles, both at the trajectory level and the traffic flow level. At the trajectory level, Przybyla established a dynamic car-following model for driving distraction [24]. At the traffic flow level, interference has an impact on vehicle speed [25] and further influences intersection capacity [26–28].

The mechanism of the trajectory and emission characteristics affected by interference has not been fully understood. Further investigation is thus necessary. Hence, this article was aimed at quantifying the impact of violations on emissions at intersections. The content of this article is divided based on the following two aspects. (1) Variations in vehicle operating affected by violations. Variations of vehicle headways and trajectories are analyzed based on manual investigation data. (2) Based on the analysis above, increased emissions of vehicles affected by violations included two levels: (a) modeling at the trajectory level for second-by-second activities of the first four affected vehicles and (b) modeling at the traffic flow level for the aggregated

parameters (number of stops and idling time) of the subsequent vehicles after the first four vehicles. A numerical simulation is conducted to assess the impact of violations on emissions based on the existing study.

2. Materials and Methods

In this study, violations are defined as the behavior that will block the vehicle fleet. Pedestrians and cyclists are the objectives of violations.

Increased emissions of vehicles affected by violations include two levels (see Figure 2): (1) trajectory level for the first four affected vehicles and (2) traffic flow level for the subsequent vehicles. At the trajectory level, the study focused on second-by-second activities of the first four affected vehicles. First, the trajectory model of the first affected vehicle is developed. Then, the trajectory of the other three vehicles is constructed by using the Gipps car-following model. At the traffic flow level, a linear emission model that can describe the relationship between emission factors and idling time in the one-stop and two-stop scenarios is developed by using Global Position System (GPS)-collected data at 44 intersections in Beijing. Increased emissions are calculated by the number of stops and idling time before and after violations based on the linear emission model. Finally, a case study is conducted to assess the impact of violations on vehicle emissions at signalized intersections.

2.1. Data Collection. This article includes two types of data. (1) Manual investigation data are used for describing the vehicle operating characteristics under violation. (2) Emission data are used for developing the linear emission model, which can explain the relationship between emission factors and idling time in the one-stop and two-stop scenarios.

2.1.1. Manual Investigation Data. Video data of 8 signalized intersections under mixed traffic were collected in Beijing, China, which are used to model the operating of vehicles affected by violations. The data include intersection attributes and violation data.

(1) Intersection attributes

(a) Channelization information
(b) Signal information

(2) Violation data: Violation data were acquired from videos frame by frame, which included three parts.

(a) Trajectories data. The crosswalk grid is constructed by crosswalks in the four directions of the intersection (see Figure 3). Based on the crosswalk grid in the video, positions of vehicles at each time step are collected, and 10 groups of trajectories are collected under the influence of violations.

(b) Headway. 171 groups of time headway are collected from video, and each group includes five headways of vehicle fleet after the violation with a precision of 0.02 s.

(c) Idling time of the first affected vehicle. The time precision is 0.02 s, and 66 groups of data are collected.

2.1.2. Emission Data. The emission data includes two parts.

(1) Emission rate. Vehicle emission data are derived from the local emission rate model for light-duty gasoline vehicles [29, 30]. The emission standard of China IV was selected to provide the emission rates for LDVs, which is more common in Beijing compared with other emission standards.

(2) Global positioning system (GPS) trajectory data. 1666 valid trajectories of data, whose range is 200 meters of the intersection radius, were selected from 44 arterial and collector intersections in Beijing. Vehicle specific power (VSP, kW/ton) is estimated after data quality control [31]. Other details about the data are listed as follows:

(i) Date, from April 25th, 2004, to April 16th, 2013;

(ii) Time, from 5:00 to 23:00; and

(iii) Speed, from 0 to 133 km/h (for the whole trajectory to ensure accuracy of the GPS device), with a precision of 0.1 km/h [32].

2.2. Variations of Vehicle Operating Affected by Violations. Increased emissions of vehicles affected by violations included two levels: (1) trajectory level for the first four affected vehicles and (2) traffic flow level for the subsequent vehicles. At the trajectory level, the study focused on second-by-second activities of the first four affected vehicles. At the traffic flow level, the study focused on the number of stops and idling time before and after violations of the subsequent vehicles after the first four vehicles. Increased emissions of the two levels are the total increased emissions under the violation condition.

The characteristics of headway under violations are shown in Figure 4. When the violation occurs, the headway of the first affected vehicle will increase obviously. From the first affected vehicle to the fourth, the headways gradually return to be stable. The impact of violations on the vehicle fleet disappears after the fourth vehicle. As a result, the first four vehicles are determined as vehicles affected by violations in the trajectory level.

$$t_{\text{lost}} = \sum_{i=1}^{4} \left(t_{\text{head,after},i} - t_{\text{head,before},i} \right), \tag{1}$$

where t_{lost} (s) is the total lost time of violation behaviors. i is the i^{th} vehicle after the violation location. $t_{\text{head,after}}$ (s) is the headway after the violation, and $t_{\text{head,before}}$ (s) is the time headway before the violation.

Vehicles trajectories under the violation are shown in Figure 5. The x-axis is time, and the y-axis is the distance. The negative y-axis is the location of the queuing vehicles, and the positive y-axis is downstream of the intersection.

The red point represents the location and time of the violation. τ is the reaction time plus braking time, and S_τ is the corresponding distance. The first affected vehicle will

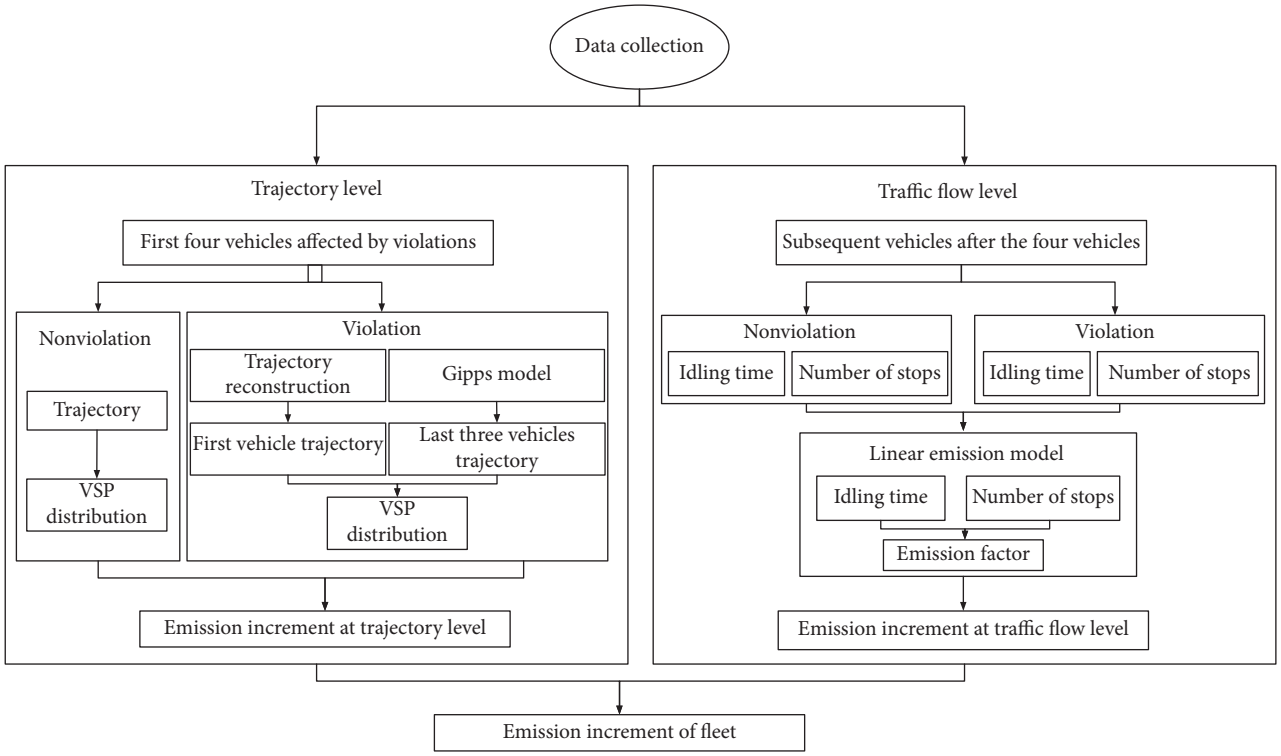

Figure 2: Overview of the methodology.

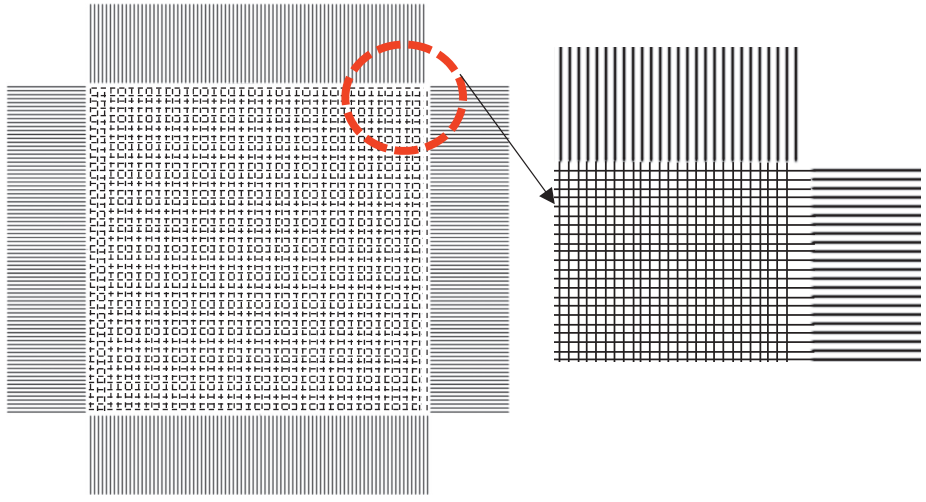

Figure 3: Intersection crosswalk grid in the video.

return to normal speed after the process of deceleration-idling-acceleration. The second vehicle starts to decelerate after the reaction time of D_r since the first affected vehicle began to decelerate. The deceleration of the second vehicle is less than the first vehicle as the interference decreases as the impact of the violation spreads in the vehicle fleet. The second vehicle begins to accelerate after the reaction time of A_r since the first affected vehicle accelerated. When the y-axis of D_r and A_r is the same, the second affected vehicle will have a second stop; the process of the second vehicle is deceleration-idling-acceleration; if not, the process is deceleration-acceleration.

The interference is gradually transmitted to the rear of the vehicle fleet, as described above. When the speed is low enough, the subsequent vehicles will extend the idling time to eliminate the interference as the fifth vehicle. Then, the subsequent vehicles will pass the intersection with the saturated time headway.

2.3. Trajectory Level. At the trajectory level, the objective is the first four affected vehicles after the violation. It is necessary to divide the model into two parts: (1) the trajectory model for the first vehicle and (2) the car-following model for the other three vehicles.

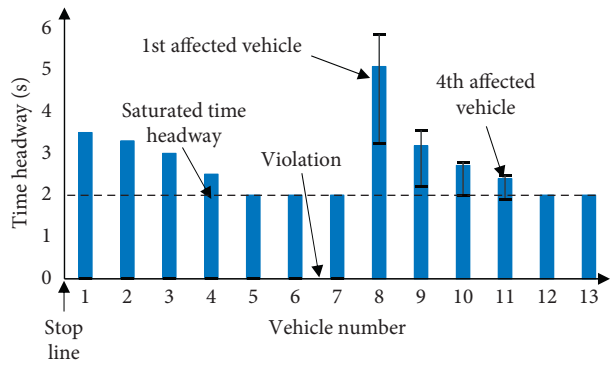

Figure 4: Time headway after violations (with the first and third quantiles).

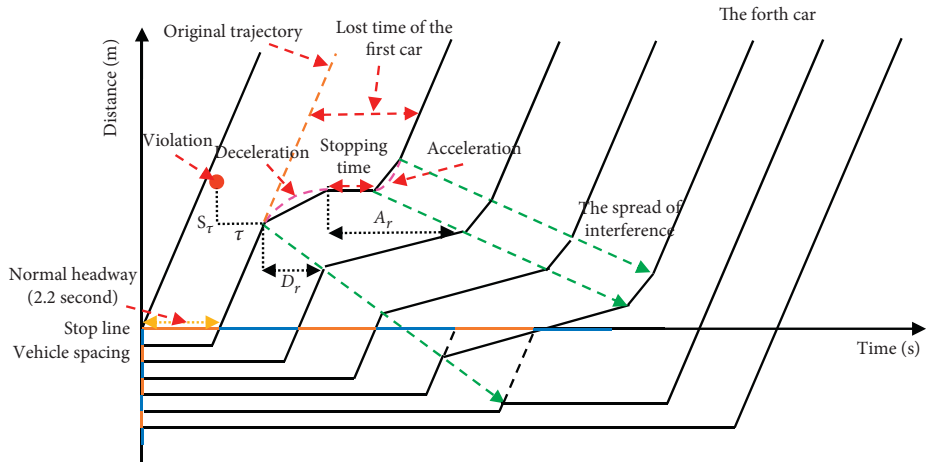

Figure 5: Vehicle trajectories affected by the violation.

2.3.1. The First Affected Vehicle. The trajectory of the first affected vehicle can be described when the following two factors are determined: (1) idling time and (2) acceleration and deceleration data.

For the idling time, sixty-six groups of idling time data in violation situations are collected. The average idling time is 2.08 s (standard deviation is 3.03).

For the acceleration and deceleration data, a corresponding relationship between vehicle speed and acceleration is developed in the low-speed range based on GPS trajectory data (see Figure 6).

As shown in Figure 6, based on the GPS trajectory data of 44 intersections, a total of 18,709 pieces of valid data of the first 10-s deceleration and 10-s acceleration around the idling time are extracted. At low speed, each speed corresponds to a group of accelerations. In other words, the process of acceleration and deceleration in violation conditions can be totally described after knowing the initial speed before violations. The acceleration of the first affected vehicle can be calculated as equations (2)–(3):

$$a_{s,t} = \text{random}\left(a_{\text{range}}\left(v_{s,t}\right)\right), \quad \text{when acceleration or deceleration,} \tag{2}$$

$$a = 0, v = 0, \quad \text{when idling,} \tag{3}$$

where $V_{s,t}$ are the speeds in the acceleration and deceleration states at time t; the states are acceleration and deceleration when s is a and d, respectively. a_{range} $(V_{s,t})$ are the corresponding acceleration range of $V_{a,t}$ and $V_{d,t}$. Each corresponding acceleration range has a database in which random values are taken by numerical simulation.

2.3.2. The Rear Three Vehicles of the First Four Affected Vehicles. The rear three vehicles decelerate after the sudden stop of the first affected vehicle. At the intersection, acceleration of the rear vehicle is closely related to the speed of the preceding vehicle, the speed of the rear vehicle, and the distance between the two vehicles. The Gipps car-following model can not only fulfill the above requirement but also generate rather realistic VSP distributions among the car-following models [33], which are calculated as equations (4)–(6):

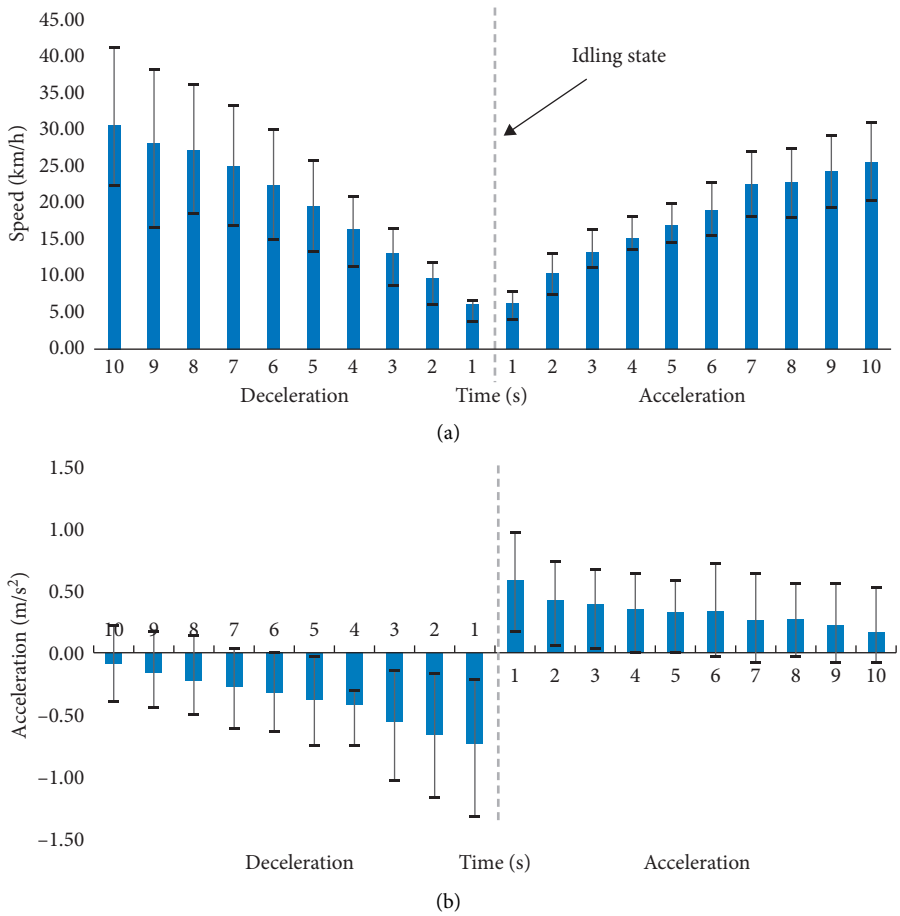

Figure 6: Speed and corresponding acceleration in the low-speed range (with the first and third quantiles). (a) Speed distribution under low-speed range of queuing. (b) Acceleration distribution under low-speed range of queuing.

$$v_n(t+\tau) = \min\left\{v_n^{\mathrm{acc}}(t+\tau), v_n^{\mathrm{dec}}(t+\tau)\right\}, \tag{4}$$

$$v_n^{\mathrm{acc}}(t+\tau) = v_n(t) + 2.5 \cdot a_n \tau\left(1 - \frac{v_n(t)}{v_n^d}\right)\sqrt{0.025 + \frac{v_n(t)}{v_n^d}}, \tag{5}$$

$$v_n^{\mathrm{dec}}(t+\tau) = -\tau d_n + \sqrt{\tau^2 d^2 + d_n\left\{2 \cdot \left[x_{n-1}(t) - x_n(t) - S_{n-1}\right] - \tau v_n(t) + \frac{v_{n-1}(t)^2}{d_{n-1}}\right\}}. \tag{6}$$

where a_n (m/s^2) is the maximum desired acceleration of the following vehicle; d_n (m/s^2) is the maximum desired deceleration of the following vehicle; $\widetilde{d}_{n-1}$ (m/s^2) is the estimation of the maximum desired deceleration of the leading vehicle; T (s) is the apparent reaction time; S_{n-1} is the effective length of a vehicle, which consists of the vehicle length and the minimum distance between the vehicles; θ is the additional delay for braking, which is 0.5; and α, β, and γ are parameters, which are 2.5, 0.025, and 0.5, respectively.

2.3.3. Emission Increment at Trajectory Level. At the trajectory level, the study focused on second-by-second activities of the first four affected vehicles. Two different models are developed: one is the trajectory model of the first vehicle, while the other is the Gipps car-following model of the three rear vehicles. The trajectory model of four vehicles affected has been developed above; thus, increased emission factors of the four vehicles can be calculated as follows:

$$\mathrm{EF}_{\mathrm{increased,trajectory},x} = 3600 \cdot \left(\frac{\sum_i \mathrm{ER}_i \cdot \mathrm{VSPBin}_{i,\mathrm{trajectory},x}}{v_{\mathrm{effected},x}} - \frac{\sum_i \mathrm{ER}_i \cdot \mathrm{VSPBin}_{i,\mathrm{normal},x}}{v_{\mathrm{normal},x}}\right), \quad x = 1, 2, 3, 4, \tag{7}$$

where $EF_{increased,trajectory,x}$ (g/km) is the increased emission factors of the x^{th} affected vehicle, VSP $Bin_{i,trajectory,x}$ is the time fraction in the i^{th} VSP bin of trajectory after violations, and $V_{effected,x}$ (km/h) is the average speed after violations.

2.4. Traffic Flow Level. At the traffic flow level, a linear emission model that can describe the relationship between emission factors and idling time in the one-stop and two-stop scenarios is developed by using GPS-collected data at 44 intersections in Beijing. Increased emissions are calculated by the number of stops and idling time before and after violations based on the linear emission model.

2.4.1. Linearly Emission Model. In this section, a linear emission model which can describe the relationship between emission factors and idling time in the one-stop and two-stop scenarios is developed. The emission model is developed based on the emission rate data and 85 VSP distributions, which are constructed based on the number of stops and idling time.

(1) VSP Distribution. Based on field measurements from the available research on emissions, there are three typical trajectories for a vehicle passing through an intersection (see Figure 7): (a) No stop, (b) one stop, and (c) multiple stops at the intersection (30, 31). It is hypothesized that each of these speed profiles generates different levels of emissions, with type three generating the highest amount of emission due to longer idling time and more acceleration and deceleration circles.

The equation for calculating VSP is provided by equation (8). VSP values are binned at an interval of 1 kW/ton. This article analyzes the VSP bins of −20 kW/ton to 20 kW/ton. More than 98% of the VSP data are in this range.

$$VSP_t = \frac{A \cdot v_t + B \cdot v_t^2 + C \cdot v_t^3}{m} + (a_t + g \cdot \sin\theta) \cdot v_t, \quad (8)$$

where a_t (m/s^2) is the acceleration, g (m/s^2) is the acceleration due to gravity, which is 9.8 m/s^2; and $\sin\theta$ is the road grade. A (kw·s/m), B (kw·s^2/m^2), and C (kw·s^3/m^3) are road load coefficients, representing rolling resistance, rotational resistance, and aerodynamic drag, respectively; the values of A, B, and C are 0.156461, 0.0020002, and 0.000493, respectively. m (ton) is the vehicle weight, and the value is 1.4788 ton.

Based on GPS trajectory data, idling time rarely exceeds 150 s for one-stop vehicles, or 275 s for two-stop vehicles. Thus, 85 VSP distributions are developed based on the number of stops, idling time, and division of upstream and downstream (see Table 1).

(2) Emission Rates. Vehicle emission rate data were derived from the local emission rate model for light-duty gasoline vehicles (see Figure 8), and the type of gasoline emission standard is China IV.

(3) Emission Factors. Idling time and number of stops are the most important changes under the violation. Therefore, the eimssion factors have two key parameters: number of stops and the idling time based on GPS data (see Figure 8). The

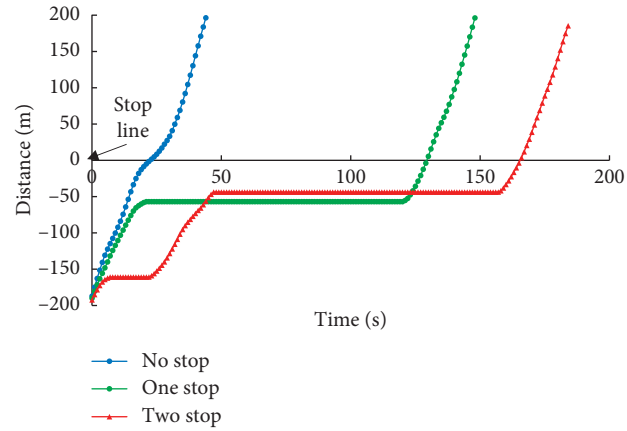

Figure 7: Three types of GPS trajectories at mixed-flow intersection.

Table 1: Information of the eighty-five VSP distributions.

Serial number	Spatial position	Number of stops	Idling time (s)
1	Downstream of intersection	0	0
2	Upstream of intersection	0	0~2
3	Upstream of intersection	1	2~5
4	Upstream of intersection	1	5~10
5	Upstream of intersection	1	10~15
.....			
30	Upstream of intersection	1	135~140
31	Upstream of intersection	1	140~145
32	Upstream of intersection	1	145~150
33	Upstream of intersection	2	10~15
34	Upstream of intersection	2	15~20
35	Upstream of intersection	2	20~25
.....			
83	Upstream of intersection	2	260~265
84	Upstream of intersection	2	265~270
85	Upstream of intersection	2	270~275

downstream emission factor is constant, as there is no stop. The emission factors are calculated as follows:

$$EF_v = \frac{3600 \cdot \sum_i ER_i VSPBin_i}{v}, \quad (9)$$

where EF_v (g/km) is the emission factor at the average speed of v (km/h). ER_i (g/s) is the mean emission rate of the i^{th} VSP Bin. VSP Bin_i is the fraction in the i^{th} VSP Bin.

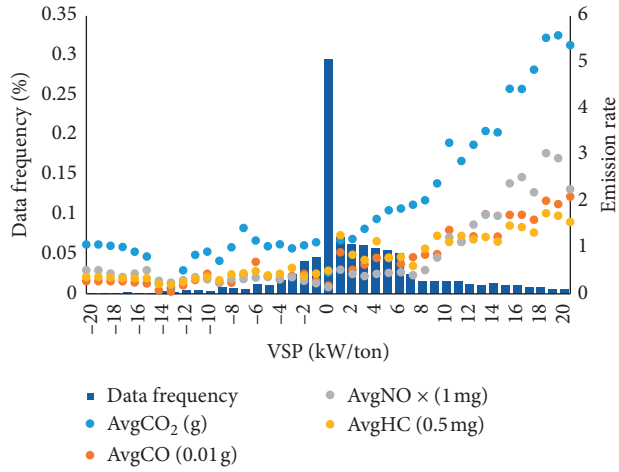

Figure 8: Mean emission rates in each VSP bin.

The emission factors increase linearly with the increase in idling time, as shown in Figure 9. The difference in emission factors between one-stop and two-stop vehicles is small under the same idling time. It is because the two-stop vehicle keeps a low speed and low acceleration, while the corresponding VSP value is concentrated around zero, and the corresponding emission rate is also small. But the range of the idling time of one-stop and two-stop vehicles is obviously different. The emission factor model is shown as follows:

$$\mathrm{EF}_{c,i} = a_{c,i} \cdot t_{\mathrm{idling}} + b_{c,i}, \quad c = 1, 2, i = 1, 2, 3, 4, \tag{10}$$

where EF_i, EF_j (g/km) are emissions of types i and j. When $i = 1$, 2, 3, 4, EF_i is the emission factor of CO_2, CO, NO_X, and HC of one-stop vehicles, respectively. When $c = 1$, 2, EF_j is the emission factor of one-stop and two-stop vehicles, respectively. t_{idling} is the idling time of the vehicle. a_i and b_i are parameters.

2.4.2. Variations of Vehicles Operating at Traffic Flow Level. At the traffic flow level, the study focused on the number of stops and idling time for the subsequent vehicles after the first four vehicles, which is divided into two scenarios (see Figure 10).

(1) Unsaturated condition of the vehicle fleet after being disturbed by violations;

(2) Saturated condition of the vehicle fleet after being disturbed by violations.

As shown in Figure 10, the total lost time of the first four affected vehicles is 4 s in the unsaturated condition. The idling time of subsequent vehicles increases by 4 s, and the number of stops is still one. Under the saturated condition, two vehicles will transform from one stop to two stops due to the increased idling time. And the idling time of two-stop vehicles increases by 4 s. Suppose that the maximum number of stops for all vehicles is two. Subsequent vehicles are divided into three types: (type A) one-stop vehicle, the increase in idling time is equal to the total lost time, (type B) transformation from one-stop vehicle to two-stop vehicle, and (type C) two-stop vehicle, the increase in idling time is equal to the total lost time of cycles.

Under the unsaturated condition, the subsequent vehicles are all type A. Under the saturated condition, vehicles that passing through the intersection are types A, B, and C at the beginning. As cycles pass, type A vehicles will disappear first, followed by type B vehicles. After all vehicles transform to two-stop vehicles, vehicles passing through the intersection are all type C.

As shown in Figure 11, VSP distributions of vehicles with and without violations are divided into three conditions, which corresponds to types A, B, and C (see Figure 11). For types A and C, the number of stops of affected vehicles is constant. Thus, the difference in VSP distributions of vehicles with and without violations is small. For type B, the number of stops transforms from one to two, and the idling time increment is the sum of the lost time and the red-light time. The frequency of VSP distributed above 0 kW/ton will be much highly affected by violations.

Take equation (10) as a reference. The emission model has been developed based on the number of stops and idling time. The operation change of subsequent vehicles, which are after the first four affected vehicles, is reflected in the number of stops and idling time. Therefore, increased emissions of the subsequent vehicles can be obtained by the emission model above. Based on equation (11), the numerical simulation method is used to calculate the emissions under violation conditions.

$$\begin{aligned}\mathrm{EF}_{\mathrm{increased,flow},y} = &\left(a_{\mathrm{cAfter},i} \cdot t_{\mathrm{after}} + b_{\mathrm{cAfter},i}\right) \\ &- \left(a_{\mathrm{cBefore},i} \cdot t_{\mathrm{before}} + b_{\mathrm{cBefore},i}\right),\end{aligned} \tag{11}$$

where $\mathrm{EF}_{\mathrm{increased,flow},y}$ (g/km) is the increased emission factors of subsequent vehicles. y is the y^{th} vehicle of vehicles going through the intersection in the cycle. t_{after} is the idling time after violations, and t_{before} (s) is the idling time without violations. cAfter and cBefore are stopping numbers before and after violations, respectively.

2.5. Increased Emissions Affected by Violations. The analysis of emissions affected by violations includes two levels. At the trajectory level, the study focused on second-by-

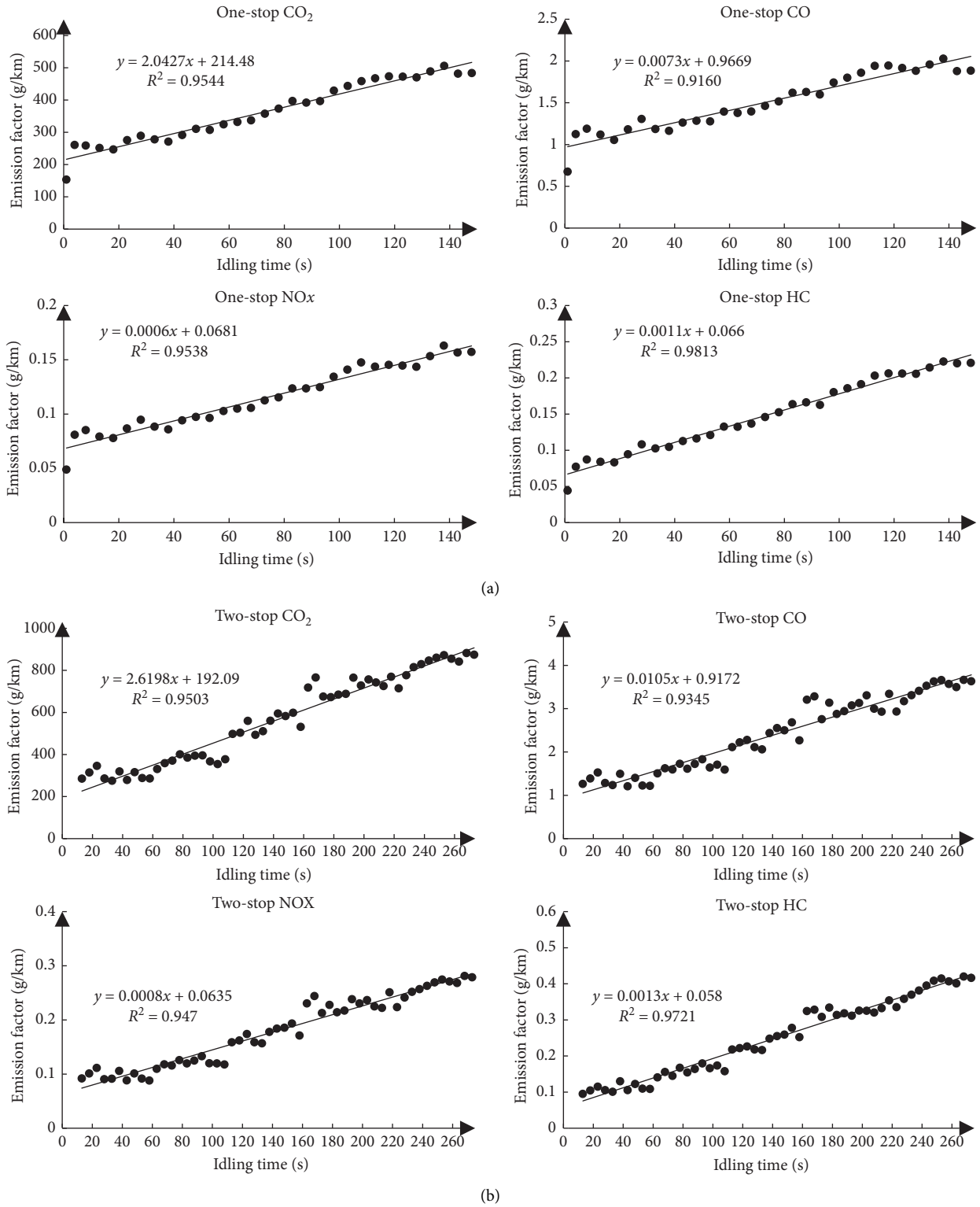

Figure 9: Emission factor model based on the number of stops and idling time.

second activities of the first four affected vehicles. At the traffic flow level, the study focused on the aggregated parameters (number of stops and idling) for the subsequent vehicles after the first four vehicles, and the conditions are divided into two categories: unsaturated and saturated conditions of the vehicle fleet disturbed by violations.

The sum of the increased emissions on these two levels is the total emission at intersections affected by violations, which can be calculated as follows:

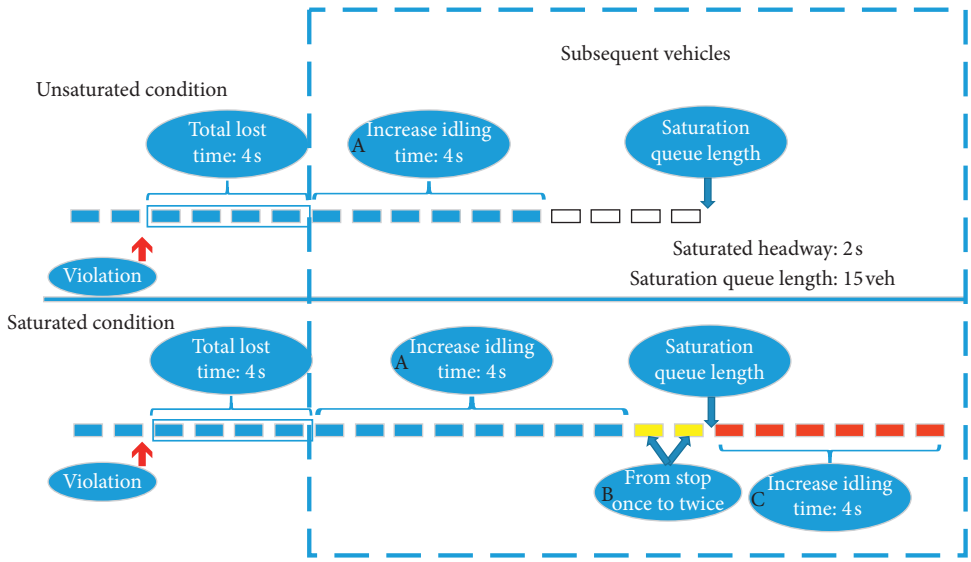

Figure 10: Characteristics of subsequent vehicles after violations.

$$\mathrm{AE} = \frac{\sum_{x=e}^{e+3} \mathrm{EF}_{\mathrm{increased,trajectory},x} + \sum_{x=e+4}^{n} \mathrm{EF}_{\mathrm{increased,flow},x}}{\sum_{i=1}^{n} \left(\mathrm{EF}_i + \mathrm{EF}_{\mathrm{downstream}}\right)} \cdot D, \tag{12}$$

where AE (%) is the increased emission increment of the cycle. e is the e^{th} vehicle, which is the location of the first affected vehicle. n is the vehicle number of the cycle. $\mathrm{EF}_{\mathrm{increased,trajectory},x}$ (g/km) is the increased emission factors of the first four affected vehicles. $\mathrm{EF}_{\mathrm{increased,flow},y}$ (g/km) is the increased emission factors of the subsequent vehicles after the first four affected vehicles. EF_i (g/km) is the normal emission factors of vehicles. $\mathrm{EF}_{\mathrm{downstream}}$ (g/km) is the emission factors downstream of the intersection. D (km) is the distance of the study range, which is 200 meters.

3. Case Study

Numerical simulations are designed in the case. The impact of violations on intersection emissions can be quantified based on the model built at the trajectory and traffic flow levels. The numerical simulation object of the case is the arterial (north-south) direction of the intersection. The seven simulation conditions are listed as follows:

(1) The average lost time is 5.52 s according to the violation data.

(2) Traffic flow arrival distribution conforms to Poisson distribution.

(3) The research scope is in 200 meters of the intersection.

(4) The maximum number of stops is two.

(5) The average speed of the normal vehicle at the intersection is 16.74 km/h according to the 1666 trajectories.

(6) The frequency of violations is 1 time/cycle/lane based on the actual statistics.

(7) The two objects to be compared are (1) vehicle emissions in this cycle before the violation and (2) the same vehicles after violations. The number of vehicles is the same.

3.1. Case Intersection. A typical intersection in Beijing (Anli and Huizhong North) is chosen as a reference for the case intersection, which is the arterial and collector protected intersection. The simulation object is the arterial (north-south) direction of the intersection. The signal information and channelization information are shown in Table 2.

3.2. Results and Discussion. When the volume is 38 veh/lane/cycle, for example, emission increment under violations in the case study is as shown in Figure 12 The x-axis indicates the cycle number, and the y-axis indicates the emission increment under the impact of violations. VSN means "the number of stops of vehicles is increasing after violations." Figure 12 explains the impact of violations on emissions at intersections under the volume from the following four aspects.

(1) The cycle number is less than 13: emission increment increases as VSN until the proportion of two-stop vehicles after violation reaches 100%.(saturated flow/(volume - saturated flow after violations) = 13).

(2) The cycle number is equal to 13: all vehicles have to stop twice after violations.

(3) The cycle number is between 13 and 26: the stopping number is two and the stopping time is increasing, the growth rate of emission after violations has a slower trend, and is even smaller than the growth rate of emission before violations.

(4) The cycle number is over 26: the three-stop vehicle will appear after violations.

Based on the analysis above, emission increment under violations in the case study is shown in Figure 13 The x-axis indicates the vehicle volume, and the y-axis indicates the

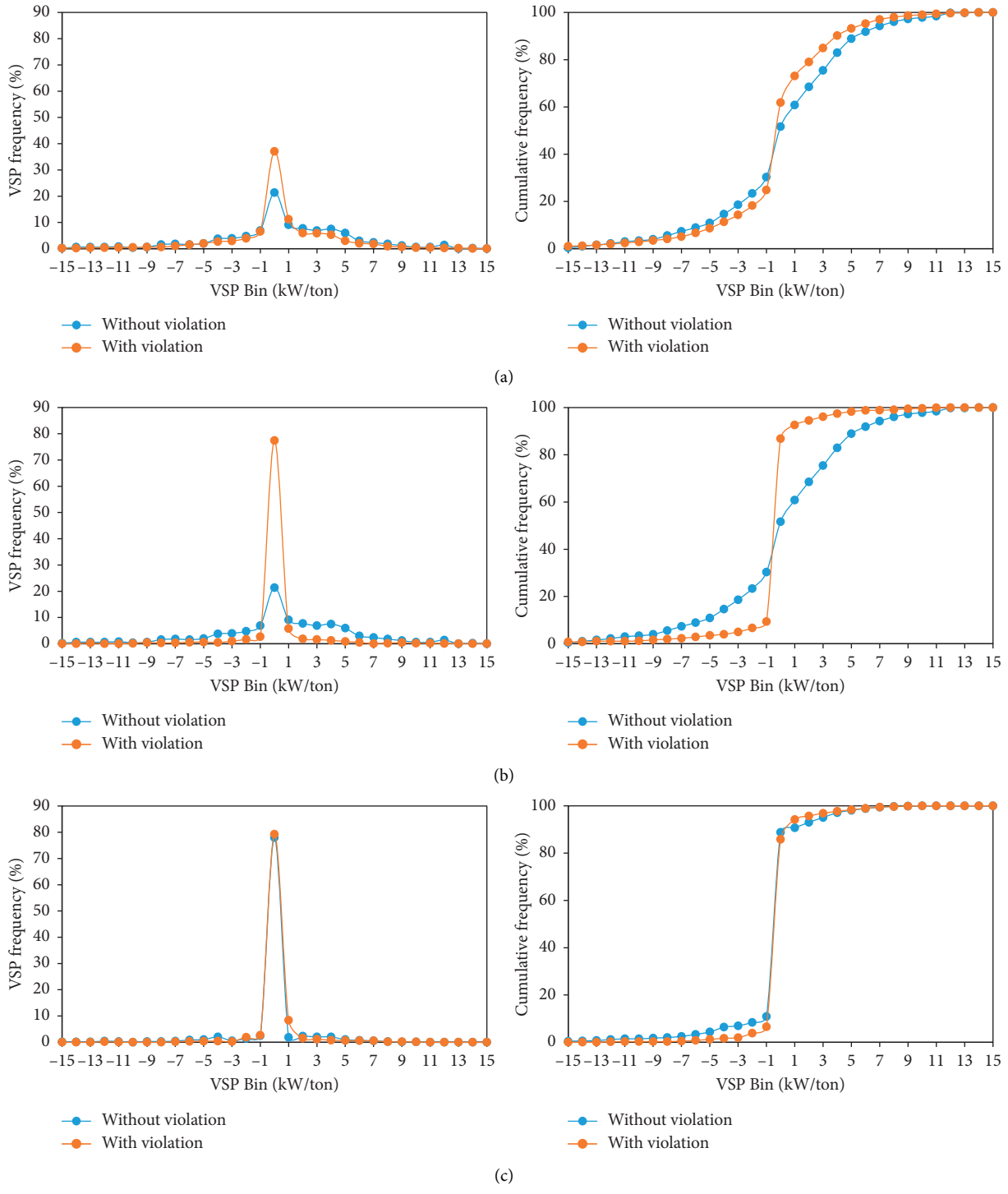

FIGURE 11: VSP distributions of vehicles with and without violations. (a) One-stop vehicle (type A). (b) The vehicle transforms from one stop to two stops (type B). (c) Two-stop vehicle (type C).

emission increment under the influence of violations. And different volumes will have different simulation cycles to avoid three-stop vehicles. Taking CO_2 as an example, the increment of CO_2 emissions can be divided into unsaturated and saturated states.

(1) Under the unsaturated condition, the emission increment is constant, and when the volume is 35 veh/lane/cycle, the emissions have barely increased (1.08%) because the stopping number is constant and the idling time only increases by 5.52 s.

Table 2: Signal and channelization information of case intersection.

Signal information (s)				Channelization information			
Phase	Green	Yellow	All red	Direction	Lane number		
North-south straight	74	3	2		Straight	Left	Right
North-south turn left	42	3	2	North	3	1	1
East phase	34	3	2	South	3	1	Straight-right
West phase	28	3	2	East	0	1	Straight-right
Cycle time		198		West	1	1	Straight-right

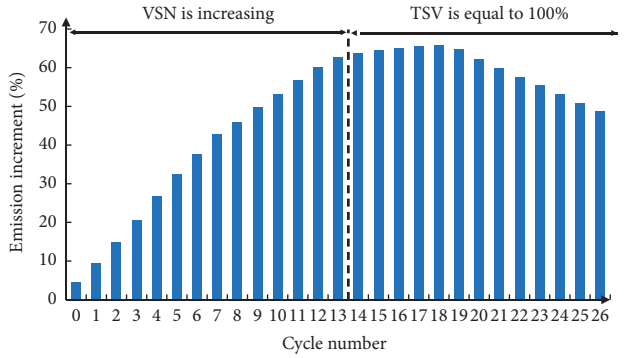

Cycle time (s)	Green time (s)	Lost time (s)
198	74	5.52
Volume (veh/cycle)	Saturated flow (veh/cycle)	Saturated flow after violations (veh/cycle)
38	37	35

Figure 12: Emission increment after violations such as cycle passing (volume = 38 veh/lane/cycle).

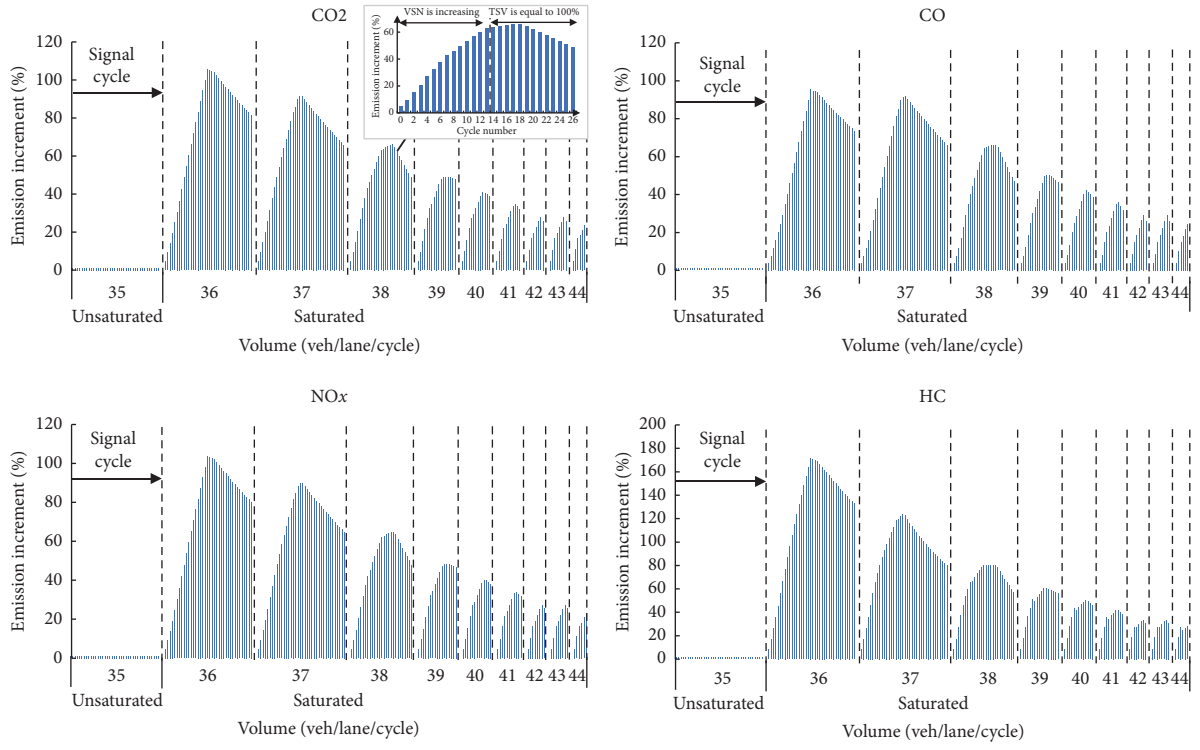

Cycle time (s)	Green time (s)	Saturated flow (veh)	Saturated flow after violations (veh)
198	74	37	35

Figure 13: Emission increment after violations for saturated/unsaturated conditions as cycle passing.

(2) Under the saturated condition, the emission increment increases sharply as the one-stop vehicle gradually transforms to the two-stop vehicle because of violations. As the proportion of two-stop vehicles after violations reaches 100%, and as the proportion before violations keeps increasing, the increment of emissions will decrease steadily. At the ninth cycle (half an hour), the emission increment is changed from 45% to 33% as the volume is changed from 36 to 42 veh/lane/cycle.

(3) As the cycle passes, the increment emissions of violations will have another increasing-decreasing process when three-stop vehicles appear. And a more increasing-decreasing process will appear when multiple-stop vehicles appear.

4. Conclusions

This paper studies the impact of violations on emissions at intersections based on the real-world driving trajectory data. First, the characteristics of vehicle operating affected by violations are analyzed. Second, a violation emission model is developed to evaluate emission increment under trajectory and traffic flow levels. Finally, a numerical simulation is conducted to assess the impact of violations on emissions based on the existing study. The main findings from the research can be summarized as follows.

The headway stabilized by the fourth affected vehicle, and the average total lost time caused by violations is 5.52 s. The effect of violations can be divided into trajectory and traffic flow levels.

The proposed emission model under trajectory and traffic flow levels can be used for estimating the impact of violations. The trajectory is modeled by the Gipps car-following model, and the proposed linear emission model based on the number of stops and idling time is used for the traffic flow level. At the trajectory level, the first four vehicles have obvious trajectory characteristics. The operating mode of the first affected vehicle is deceleration-idling-acceleration. The other three vehicles are modeled by the Gipps car-following model. At the traffic flow level, the proposed linear emission model based on the number of stops and idling time is used for estimating the emission of subsequent vehicles.

The emission increment is constant under the unsaturated condition and is 1.08% when the volume approaches saturated flow. The emission increment increases sharply as the one-stop vehicle gradually transforms to the two-stop vehicle because of violations under the saturated condition, and the maximum emission increment reaches 45% in half an hour in the case. The increment of emissions decreases steadily as the proportion of two-stop vehicles after violations reaches 100%, and the proportion before violations keeps increasing.

More emission numerical simulations for different types and frequencies of violations are recommended for further studies. In addition, three-stops and above should be considered in high-frequency violation scenarios.

Data Availability

Previously reported emission data were used to support this study and are available at https://doi.org/10.3141/2627-08 and https://doi.org/10.3141/2570-09. These prior studies (and datasets) are cited at relevant places within the text as references [30, 32]. The manual investigation data used to support the findings of this study are included within the article.

Disclosure

This paper was submitted for presentation at the annual meeting of the 98th Transportation Research Board.

Conflicts of Interest

The authors declare that there are no conflicts of interest regarding the publication of this paper.

Acknowledgments

This research was supported by the National Key R&D Program of China (#2018YFB1600701), the Fundamental Research Funds for the Central Universities (#2018YJS081), and the Natural Science Foundation of China (NSFC) (#51678045 and 51578052). The authors are thankful to all personnel who provided technical support and helped with data collection and processing.

References

[1] R. J. Laumbach, "Outdoor air pollutants and patient health," *American Family Physician*, vol. 81, no. 2, pp. 175–180, 2010.

[2] M. Krzyzanowski, B. Kunadibbert, J. S. Chneider et al., "Health effects of transport-related air pollution," *Journal of Health Effects of Transport-Related Air Pollution*, vol. 97, no. 5, pp. 418-419, 2005.

[3] F. Khalighi and E. Christofa, "Emission-based signal timing optimization for isolated intersections," *Transportation Research Record: Journal of the Transportation Research Board*, vol. 2487, no. 1, pp. 1–14, 2015.

[4] Federal Highway Administration, *Carbon Monoxide Categorical Hot-Spot Finding*, Federal Highway Administration, Washington, DC, USA, 2017.

[5] Y. Zhang, X. Chen, X. Zhang, G. Song, Y. Hao, and L. Yu, "Assessing effect of traffic signal control strategies on vehicle emissions," *Journal of Transportation Systems Engineering and Information Technology*, vol. 9, no. 1, pp. 150–155, 2009.

[6] L. Zhang, Y. Yin, and S. Chen, "Robust signal timing optimization with environmental concerns," *Transportation Research Part C: Emerging Technologies*, vol. 29, no. 1, pp. 55–71, 2013.

[7] M. Franklin, X. Yin, R. Urman, R. Lee, S. Fruin, and R. Mcconnell, "Environmental factors affecting stress in children: interrelationships between traffic-related noise, air pollution, and the built environment," in *Proceedings of the HEI Annual Conference*, Washington, DC, USA, May 2019.

[8] J. Xing, J. Hua, and P. Hao, "Study on pedestrian crossing rate at signal-controlled intersections," *Journal of Technology & Economy in Areas of Communications*, vol. 16, no. 5, pp. 14–19, 2014, Chinese article.

[9] C. Minh and K. Sano, "Analysis of motorcycle effects to saturation flow rate at signalized intersection in developing countries," *Journal of the Eastern Asia Society for Transportation Studies*, vol. 5, pp. 1211–1222, 2003.

[10] A. Stevanovic, J. Stevanovic, K. Zhang, and S. Batterman, "Optimizing traffic control to reduce fuel consumption and vehicular emissions: integrated approach with VISSIM, CMEM, and VISGAOST," *Transportation Research Record: Journal of the Transportation Research Board*, vol. 2128, no. 1, p. 105, 2009.

[11] X. Sun, X. Chen, Y. Qi, B. Mao, and L. Yu, "Analyzing the effects of different advanced traffic signal status warning systems on vehicle emission reductions at signalized intersections," in *Proceedings of the Presented at 95th Annual Meeting of the Transportation Research Board*, Washington, DC, USA, January 2016.

[12] K. Chen and L. Yu, "Microscopic traffic-emission simulation and case study for evaluation of traffic control strategies," *Journal of Transportation Systems Engineering and Information Technology*, vol. 7, no. 1, pp. 93–99, 2007.

[13] H. Rakha and Y. Ding, "Impact of stops on vehicle fuel consumption and emissions," *Journal of Transportation Engineering*, vol. 129, no. 1, pp. 23–32, 2002.

[14] H. C. Frey, N. M. Rouphail, and H. Zhai, "Speed- and facility-specific emission estimates for on-road light-duty vehicles on the basis of real-world speed profiles," *Transportation Research Record: Journal of the Transportation Research Board*, vol. 1987, no. 1, pp. 128–137, 2006.

[15] H. Zhai, H. C. Frey, and N. M. Rouphail, "A vehicle-specific power approach to speed- and facility-specific emissions estimates for diesel transit buses," *Environmental Science & Technology*, vol. 42, no. 21, pp. 7985–7991, 2008.

[16] A. Papson, S. Hartley, and K. Kuo, "Analysis of emissions at congested and uncongested intersections with motor vehicle emission simulation," *Transportation Research Record: Journal of the Transportation Research Board*, vol. 2270, no. 1, pp. 124–131, 2012.

[17] S. Gokhale and S. Pandian, "A semi-empirical box modeling approach for predicting the carbon monoxide concentrations at an urban traffic intersection," *Atmospheric Environment*, vol. 41, no. 36, pp. 7940–7950, 2007.

[18] K. Braven, A. Abdel-Rahim, K. Henrickson, and A. Battles, *Modeling Vehicle Fuel Consumption and Emissions at Signalized Intersection. Publication KLK721*, National Institute for Advanced Transportation Technology, University of Idaho, Moscow, Idaho, 2012.

[19] M. Brosseau, S. Zangenehpour, N. Saunier, and L. Miranda-Moreno, "The impact of waiting time and other factors on dangerous pedestrian crossings and violations at signalized intersections: a case study in montreal," *Transportation Research Part F: Traffic Psychology and Behaviour*, vol. 21, pp. 159–172, 2013.

[20] G. Ren, Z. Zhou, W. Wang, Y. Zhang, and W. Wang, "Crossing behaviors of pedestrians at signalized intersections: observational study and survey in China," *Transportation Research Record: Journal of the Transportation Research Board*, vol. 2264, no. 1, pp. 65–73, 2011.

[21] X. Wang, Y. Xu, P. J. Tremont, and D. Yang, "Moped rider violation behavior and moped safety at intersections in China," *Transportation Research Record: Journal of the Transportation Research Board*, vol. 2281, no. 1, pp. 83–91, 2012.

[22] V. Perumal, S. Marisamynathan, Study on pedestrian crossing behavior at signalized intersections," *Journal of Traffic and Transportation Engineering*, vol. 2, no. 1, pp. 103–110, 2014.

[23] M. Huan, M. Yang, and B. Jia, "Modeling cyclist violation behavior at signalized intersection in China," in *Proceedings of the 2012 Fifth International Joint Conference on Computational Sciences and Optimization*, IEEE, Harbin, China, June 2012.

[24] J. Przybyla, J. Taylor, J. Jupe, and X. Zhou, "Estimating risk effects of driving distraction: a dynamic errorable car-following model," *Transportation Research Part C: Emerging Technologies*, vol. 50, pp. 117–129, 2015.

[25] L. He, "Study on traffic efficiency of illegal lane change on signal intersection," Doctoral thesis, Chang'an University, Xi'an, China 2017. (Chinese article).

[26] J. B. Zhang, L. Yu, G. Song, J. Huang, and J. Guo, "Operational characteristics of signalized under mixed traffic: case in Beijing," in *Proceedings of the Presented at 98th Annual Meeting of the Transportation Research Board*, Washington, DC, USA, January 2019.

[27] Y. Guo, Q. Yu, Y. Zhang, and J. Rong, "Effect of bicycles on the saturation flow rate of turning vehicles at signalized intersections," *Journal of Transportation Engineering*, vol. 138, no. 1, pp. 21–30, 2012.

[28] X. Liang, Z. Liu, and Q. Kun, "Capacity analysis of signalized intersections under mixed traffic conditions," *Journal of Transportation Systems Engineering and Information Technology*, vol. 2, no. 11, pp. 91–99, 2011.

[29] D. Xie, G. Song, J. Guo, J. Sun, and L. Yu, "Development and application of an online dynamic emission model for traffic networks: a case study of Beijing," in *Proceedings of the Presented at 97th Annual Meeting of the Transportation Research Board*, Washington, DC, USA, January 2018.

[30] C. Li, L. Yu, W. He, Y. Cheng, and G. Song, "Development of local emissions rate model for light-duty gasoline vehicles: beijing field data and patterns of emissions rates in EPA simulator," *Transportation Research Record: Journal of the Transportation Research Board*, vol. 2627, no. 1, pp. 67–76, 2017.

[31] Report of Overall Architecture Design and Technical Difficult of the Distribution Regular Pattern of Traffic Emissions, *Technical Report for Center for Transportation Sector Energy Reduction and Emissions Mitigation of Beijing*, Beijing Jiaotong University, Beijing, China, 2014.

[32] J. Zhang, L. Yu, J. Guo, Y. Cheng, W. He, and G. Song, "Optimized adjustment of speed resolution and time alignment data for improving emissions estimations," *Transportation Research Record: Journal of the Transportation Research Board*, vol. 2570, no. 1, pp. 77–86, 2016.

[33] H. Lu, G. Song, and L. Yu, "A comparison and modification of car-following models for emission estimation," in *Proceedings of the Transportation Research Board 95th Annual Meeting, Transportation Research Board of the National Academies*, Washington, DC, USA, January 2016.